Electronic Supplementary Material (ESI) for Journal of Materials Chemistry A.

Supporting Information

High storage capacities and separation selectivity of C2 hydrocarbons over methane in the metal-organic framework Cu-TDPAT

*Kang Liu, Dingxuan Ma, Baiyan Li, Yi Li, Kexin Yao, Zhijuan Zhang, Yu Han and Zhan Shi**

Section I. Sample Preparation

All reagents were purchased from Sigma-Aldrich or Acros and used as received. Cu-TDPAT was synthesized according to previously published methods.[1] Cu-TDPAT was prepared by mixing 2,4,6-tris(3,5-dicarboxylphenylamino)-1,3,5-triazine (H_6TDPAT) (0.030g, 0.049mmol) with $Cu(NO_3)_2 \cdot 3H_2O$ (0.164g, 0.68mmol) in 2 mL of DMA, 2 mL of DMSO, 100 µL of H_2O and 0.9 mL of HBF_4 in a small vial and heated at 85 ºC for 3 d.

Section II. PXRD Analysis

PXRD data were collected on a Rigaku D/max 2550 Powder X-ray Diffractometer.

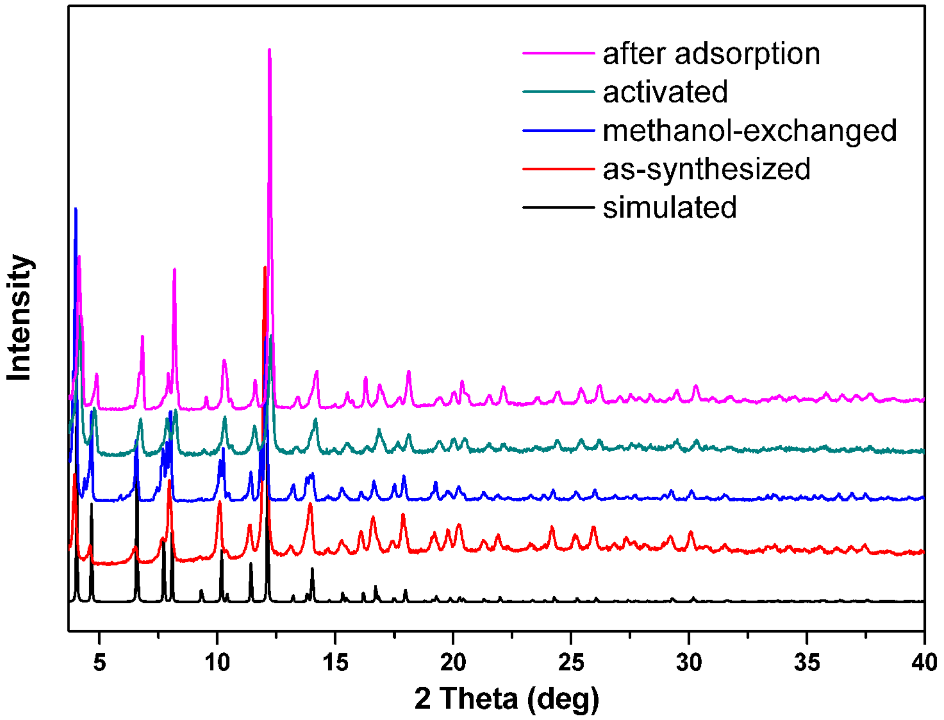

Figure S1. The PXRD data of Cu-TDPAT showing good agreement with simulated one for as-synthesized, methanol-exchanged, activated and after adsorbed sample.

Section III. Gas Sorption Measurements

Gas sorption experiments at 273K and 298K were performed on a Micrometrics ASAP 2020 surface area analyzer. Before analysis, Cu-TDPAT was soaked in methanol for 3 days with methanol refreshing every 2 hours. Then, methanol-exchanged sample was charged into a sample tube and activated at 120 °C for 10 hours by using the “outgas” function of the surface area analyzer.

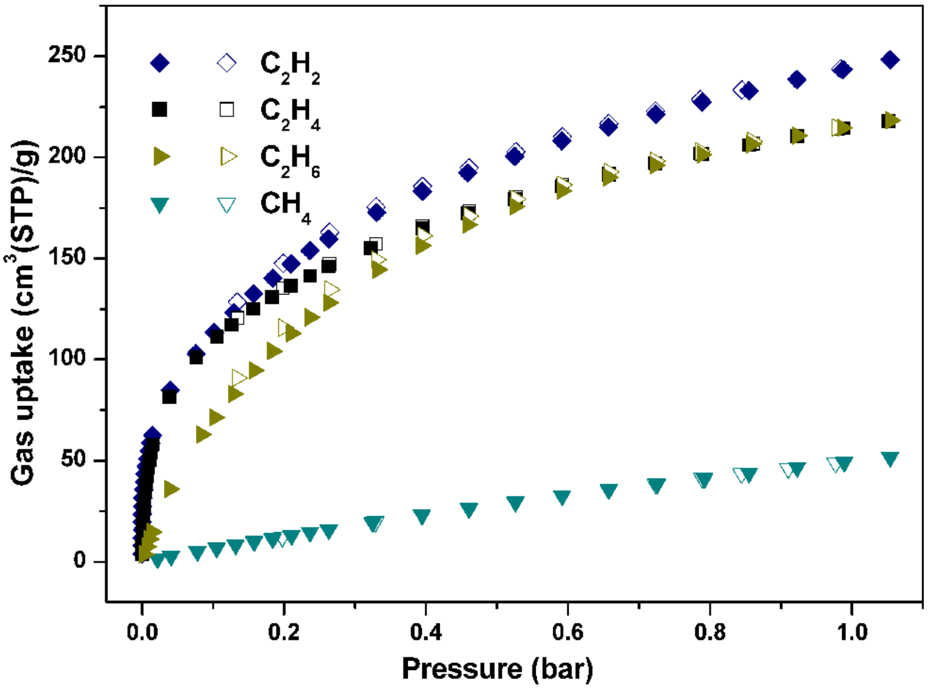

Figure S2. CH_4, C_2H_2, C_2H_4 and C_2H_6 adsorption isotherms for Cu-TDPAT at 273 K.

Section IV. Calculations of the Isosteric Heats of Gas Adsorption (Qst)

A virial-type[2] expression comprising the temperature-independent parameters a_i and b_j was employed to calculate the enthalpies of adsorption for CH_4, C_2H_2, C_2H_4 and C_2H_6 (at 273 and 298K) on Cu-TDPAT. In each case, the data were fitted using the equation: □□ □

$$\ln P = \ln N + 1/T \sum_{i-0}^{m} a_i N^i + \sum_{j-0}^{n} b_j N^j \, (1)$$

Here, P is the pressure expressed in Torr, N is the amount adsorbed in mmol/g, T is the temperature in K, a_i and b_j are virial coefficients, and m, n represent the number of coefficients required to adequately describe the isotherms (m and n were gradually increased until the contribution of extra added a and b coefficients was deemed to be statistically insignificant towards the overall fit, and the average value of the squared deviations from the experimental values was minimized). The values of the virial coefficients a_0 through a_m were then used to calculate the isosteric heat of adsorption using the following expression.

$$Q_{st} = -R \sum_{i-0}^{m} a_i N^i \, (2)$$

Q_{st} is the coverage-dependent isosteric heat of adsorption and R is the universal gas constant. The heats of varieties of gases sorption for Cu-TDPAT in this manuscript are determined by using the sorption data measured in the pressure range from 0-1 bar (273 and 298K), which is fitted by the virial-equation very well.

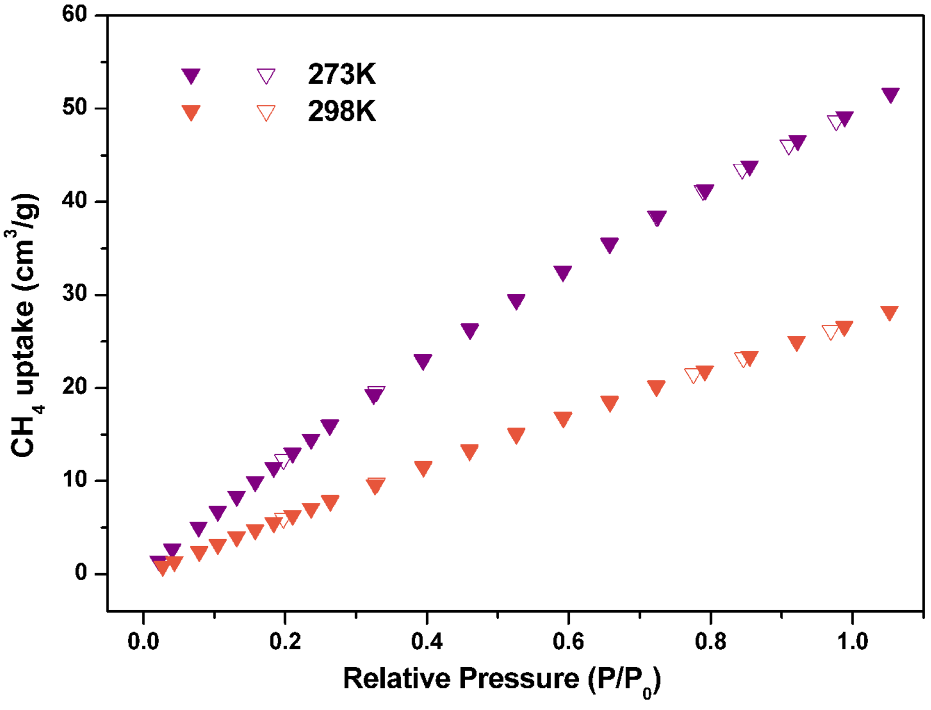

Figure S3. The CH_4 sorption isotherms for Cu-TDPAT at 273 (purple) and 298 K (orange).

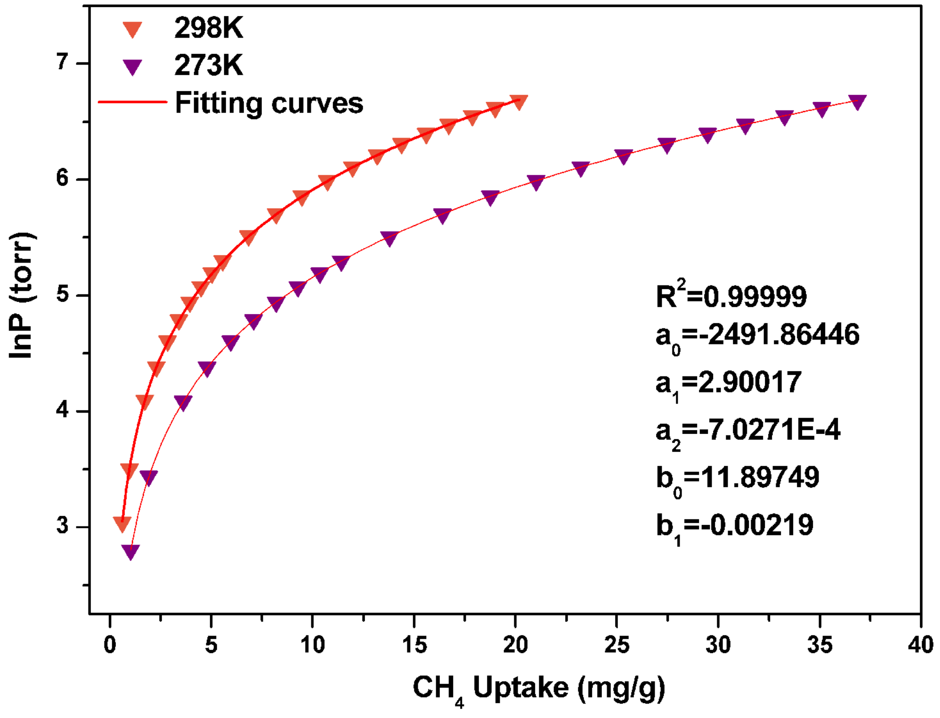

Figure S4. The details of virial equation (solid lines) fitting to the experimental CH_4 adsorption data (symbols) for

Cu-TDPAT.

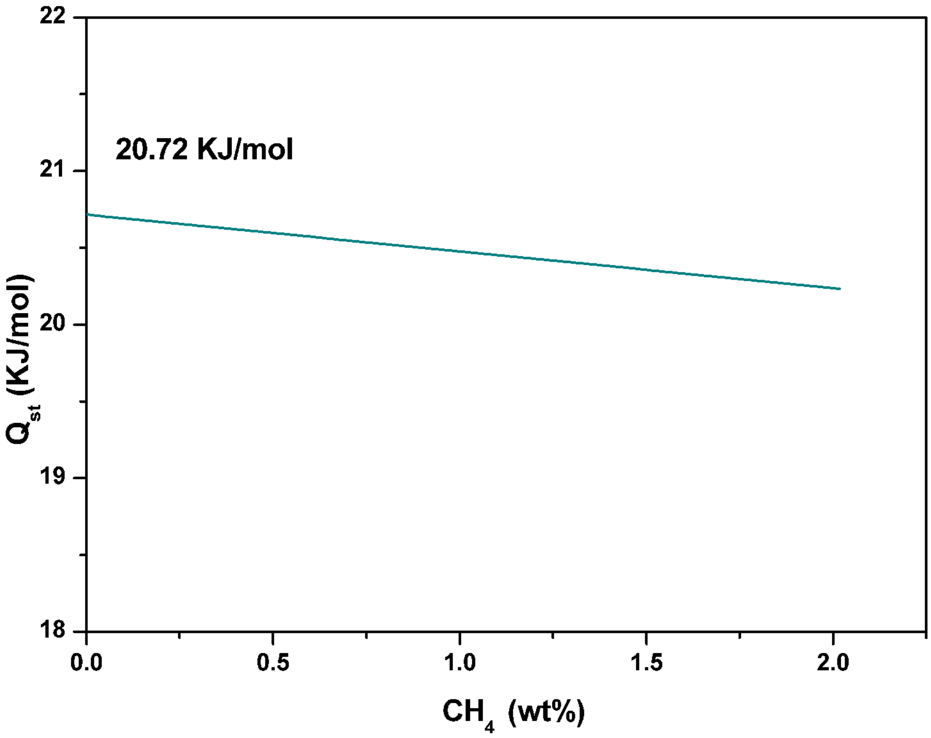

Figure S5. The CH_4 adsorption enthalpies of Cu-TDPAT.

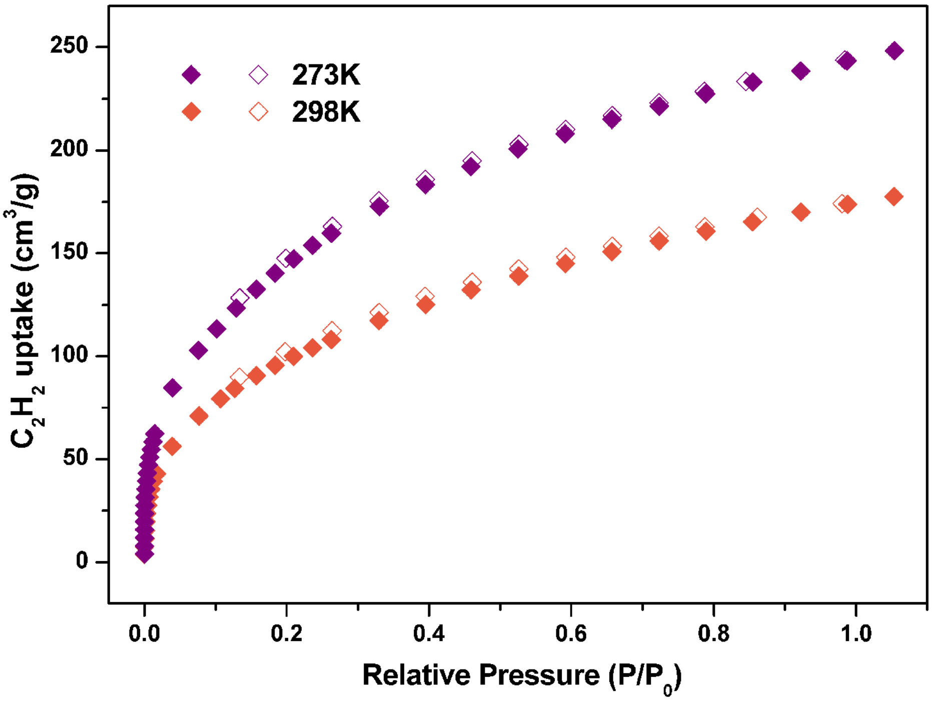

Figure S6. The C_2H_2 sorption isotherms for Cu-TDPAT at 273 (purple) and 298 K (orange).

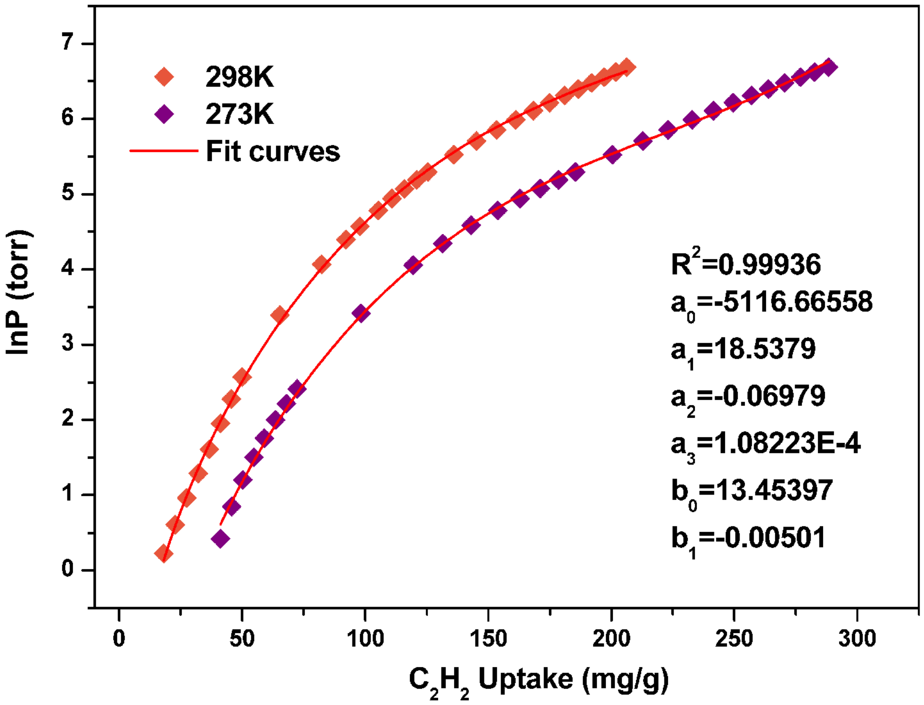

Figure S7. The details of virial equation (solid lines) fitting to the experimental C_2H_2 adsorption data (symbols) for Cu-TDPAT.

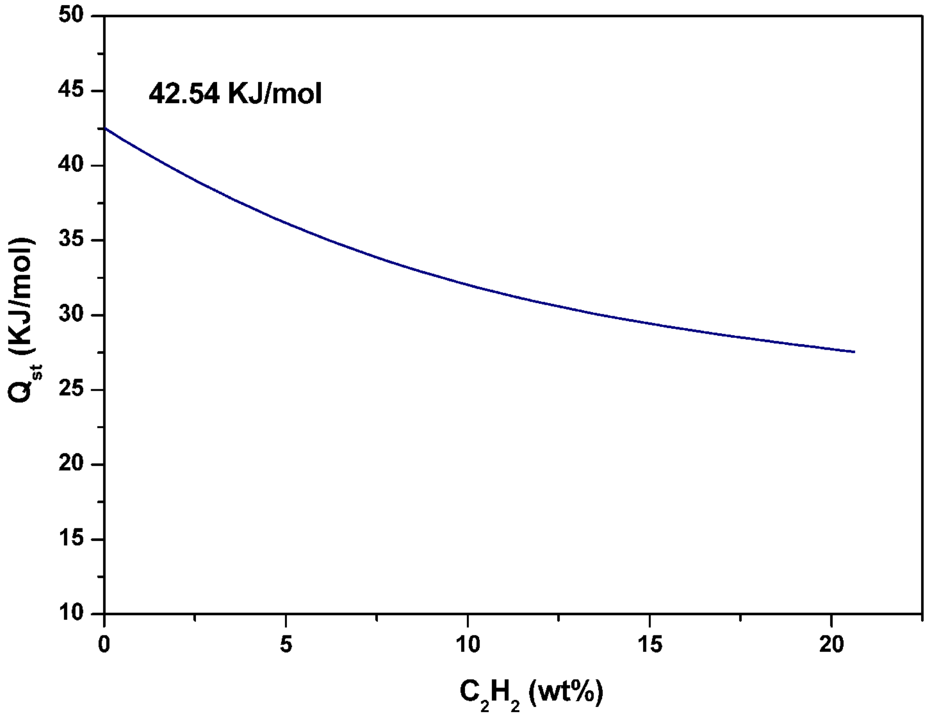

Figure S8. The C_2H_2 adsorption enthalpies of Cu-TDPAT.

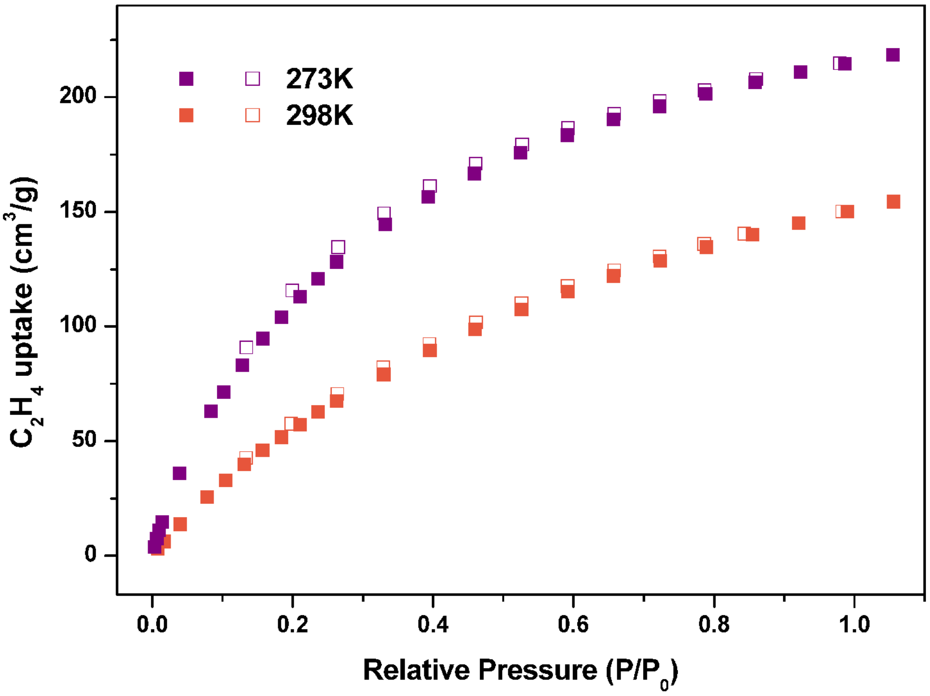

Figure S9. The C_2H_4 sorption isotherms for Cu-TDPAT at 273 (purple) and 298 K (orange).

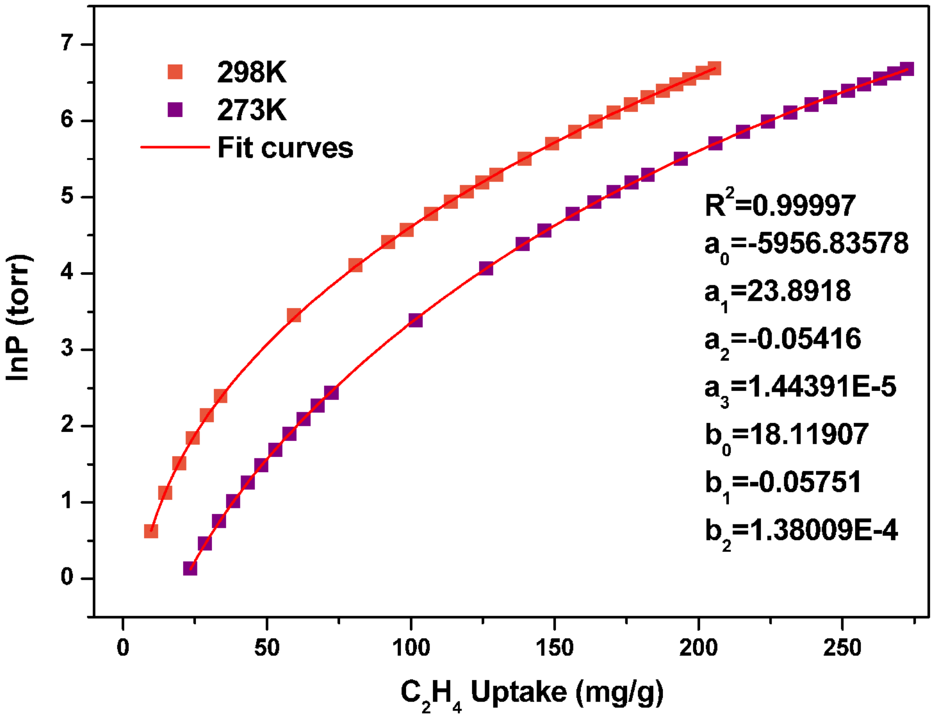

Figure S10. The details of virial equation (solid lines) fitting to the experimental C_2H_4 adsorption data (symbols) for Cu-TDPAT.

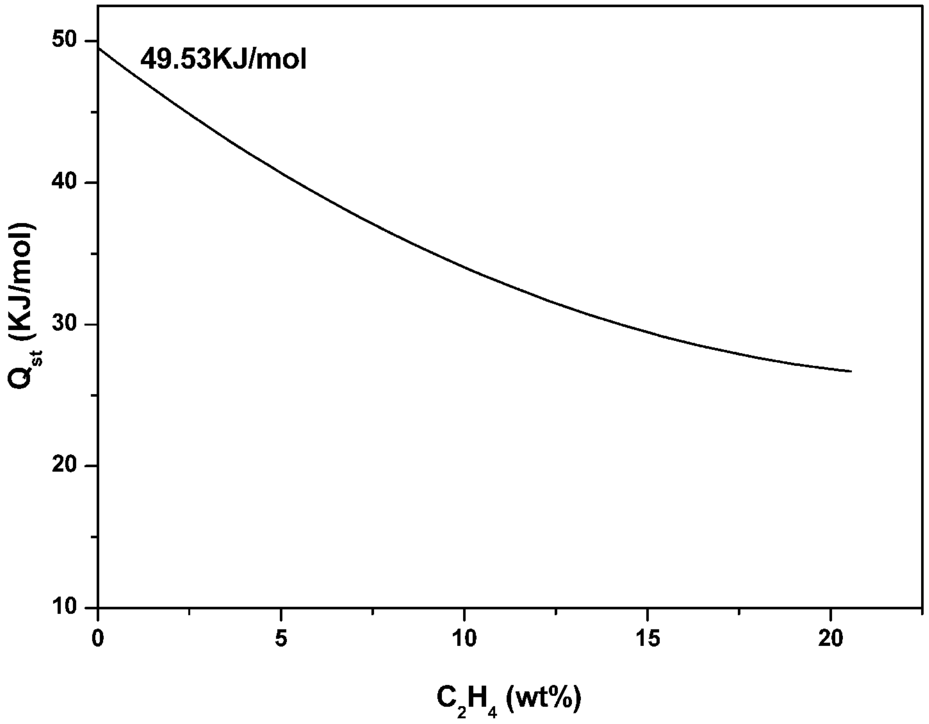

Figure S11. The C_2H_4 adsorption enthalpies of Cu-TDPAT.

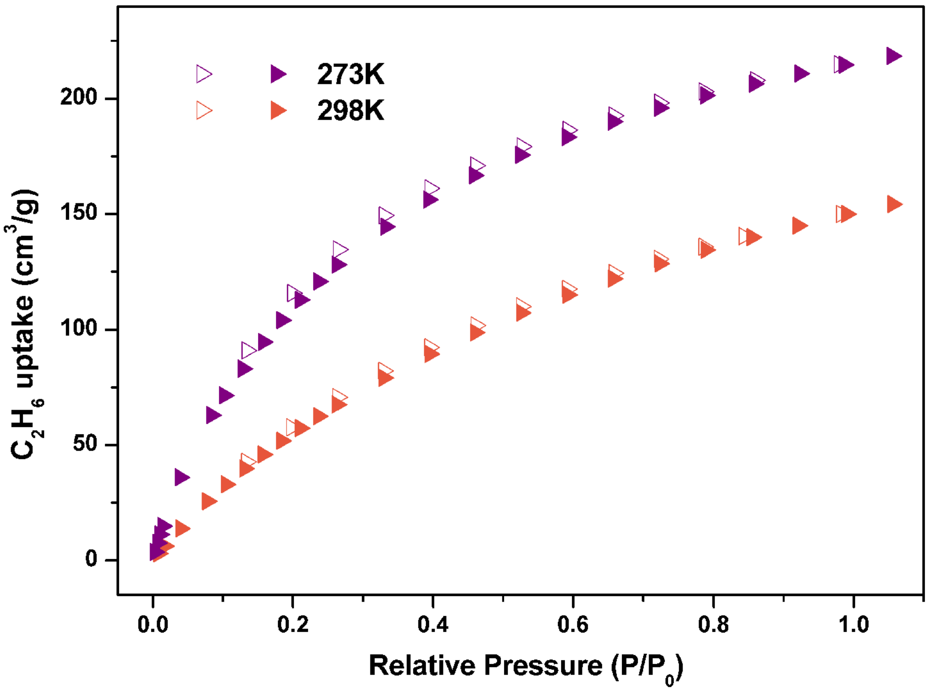

Figure S12. The C_2H_6 sorption isotherms for Cu-TDPAT at 273 (purple) and 298 K (orange).

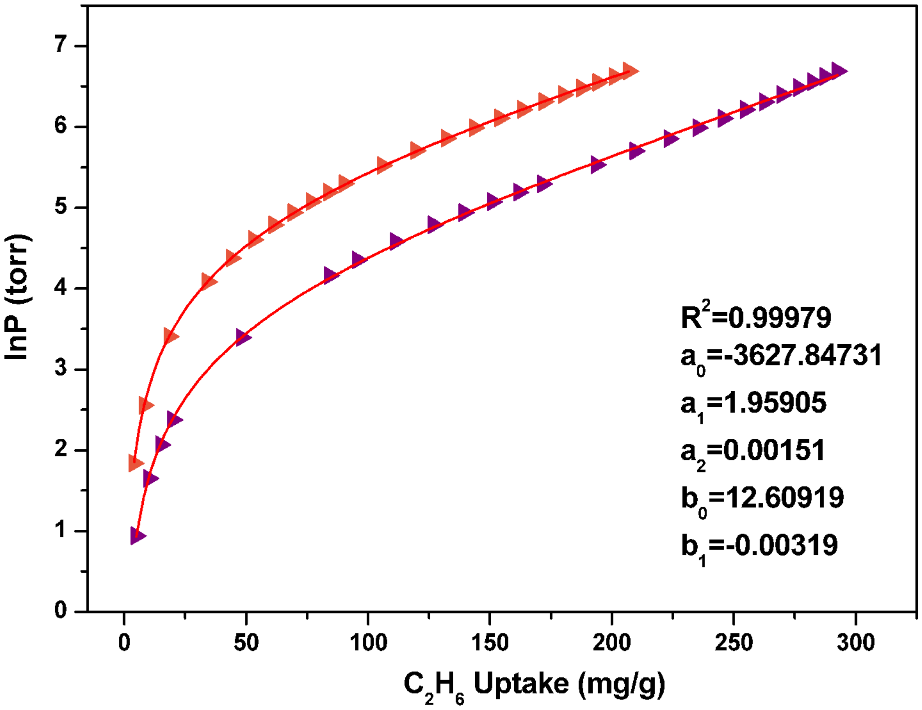

Figure S13. The details of virial equation (solid lines) fitting to the experimental C_2H_6 adsorption data (symbols) for Cu-TDPAT.

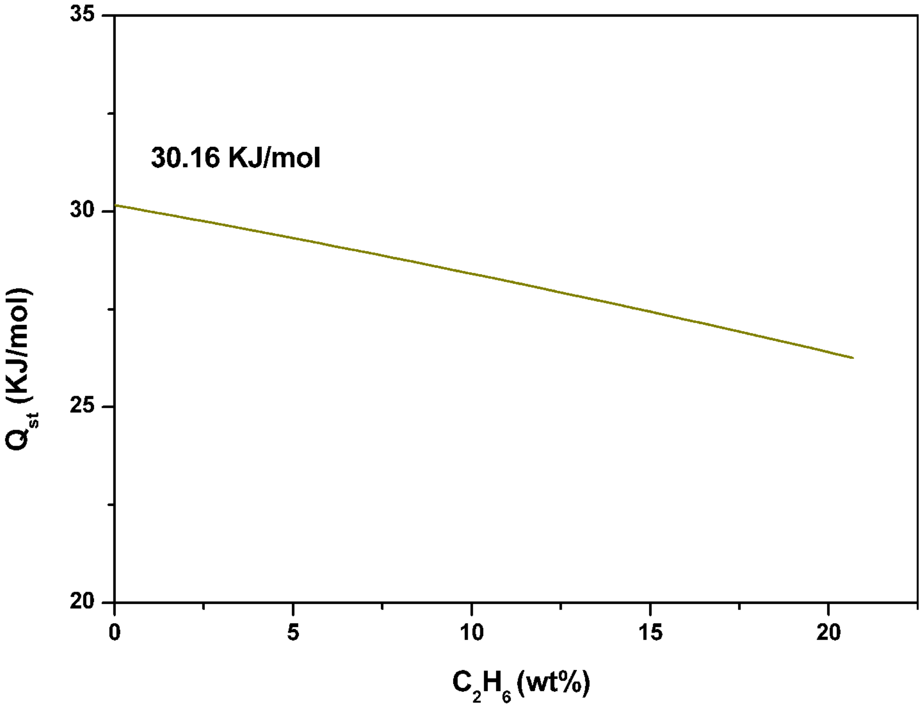

Figure S14. The C_2H_6 adsorption enthalpies of Cu-TDPAT.

Section V. Calculations of selectivities based on the Henry's Law selectivity.

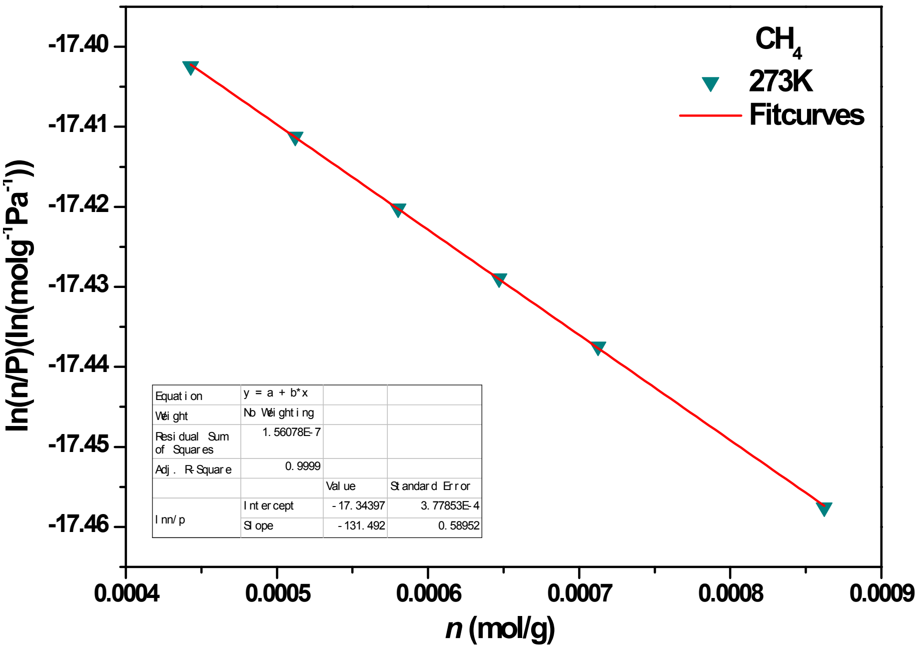

Equation	y = a + b*x		
Weight	No Weighting		
Residual Sum of Squares	1.56078E-7		
Adj. R-Square	0.9999		
		Value	Standard Error
lnn/p	Intercept	-17.34397	3.77853E-4
	Slope	-131.492	0.58952

Figure S28. Virial analysis of the adsorption data for CH_4 on Cu-TDPAT at 273 K: Low pressure data.

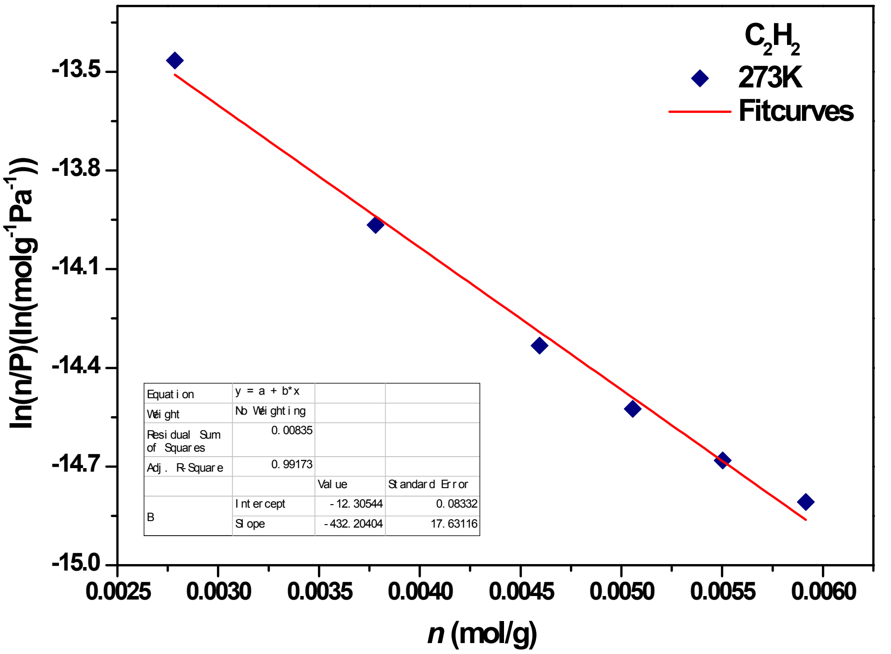

Equation	y = a + b*x		
Weight	No Weighting		
Residual Sum of Squares	0.00835		
Adj. R-Square	0.99173		
		Value	Standard Error
B	Intercept	-12.30544	0.08332
	Slope	-432.20404	17.63116

Figure S28. Virial analysis of the adsorption data for C_2H_2 on Cu-TDPAT at 273 K: Low pressure data.

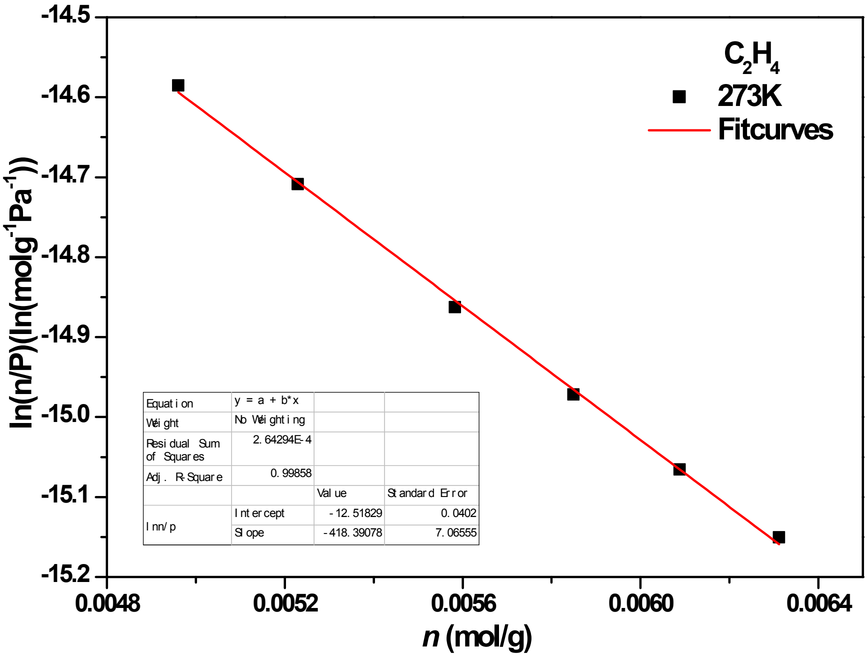

Equation	y = a + b*x		
Weight	No Weighting		
Residual Sum of Squares	2.64294E-4		
Adj. R-Square	0.99858		
		Value	Standard Error
lnn/p	Intercept	-12.51829	0.0402
	Slope	-418.39078	7.06555

Figure S28. Virial analysis of the adsorption data for C_2H_4 on Cu-TDPAT at 273 K: Low pressure data.

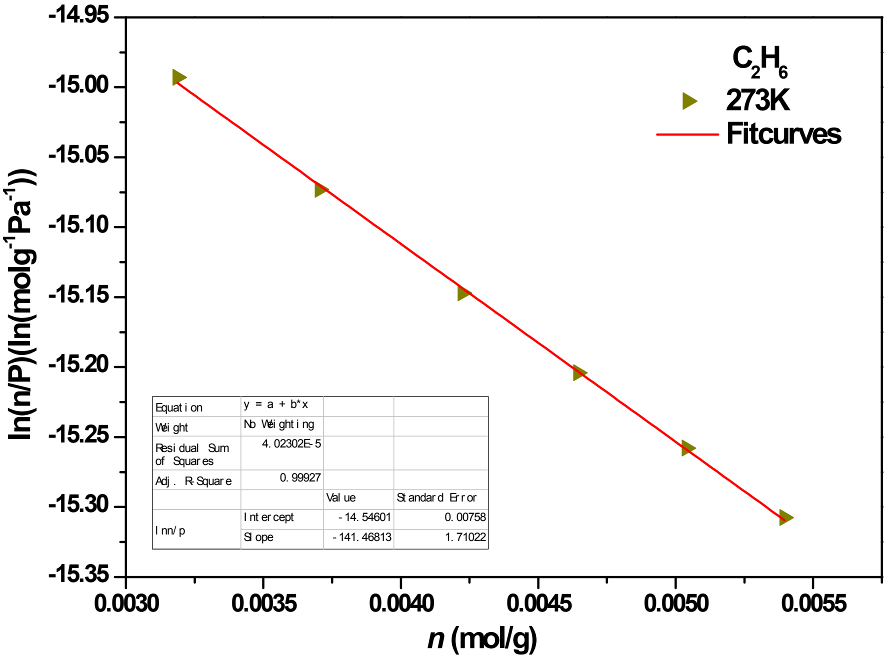

Equation	y = a + b*x		
Weight	No Weighting		
Residual Sum of Squares	4.02302E-5		
Adj. R-Square	0.99927		
		Value	Standard Error
lnn/p	Intercept	-14.54601	0.00758
	Slope	-141.46813	1.71022

Figure S28. Virial analysis of the adsorption data for C_2H_6 on Cu-TDPAT at 273 K: Low pressure data.

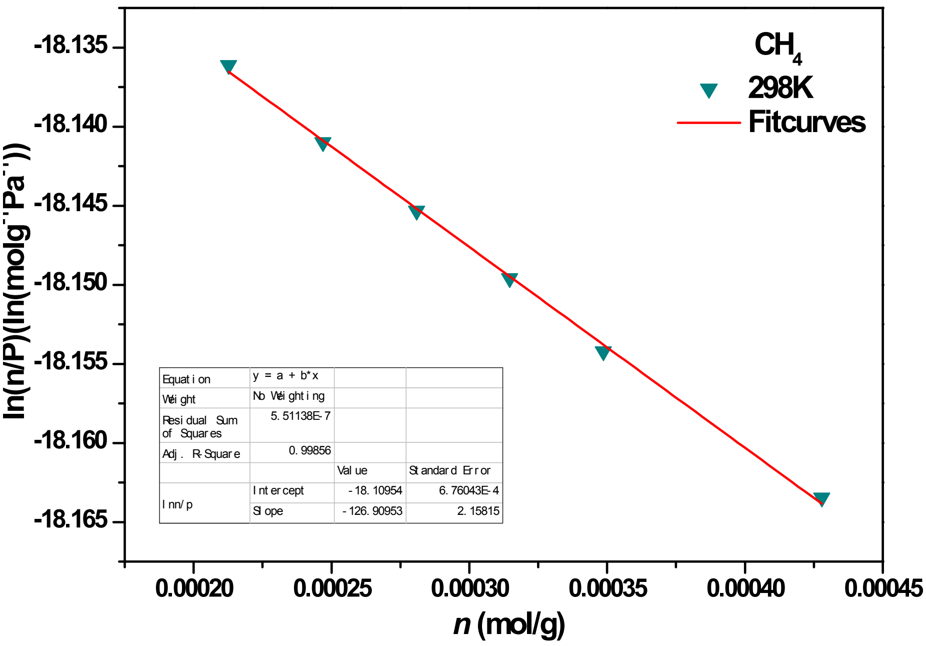

Figure S28. Virial analysis of the adsorption data for CH_4 on Cu-TDPAT at 298 K: Low pressure data.

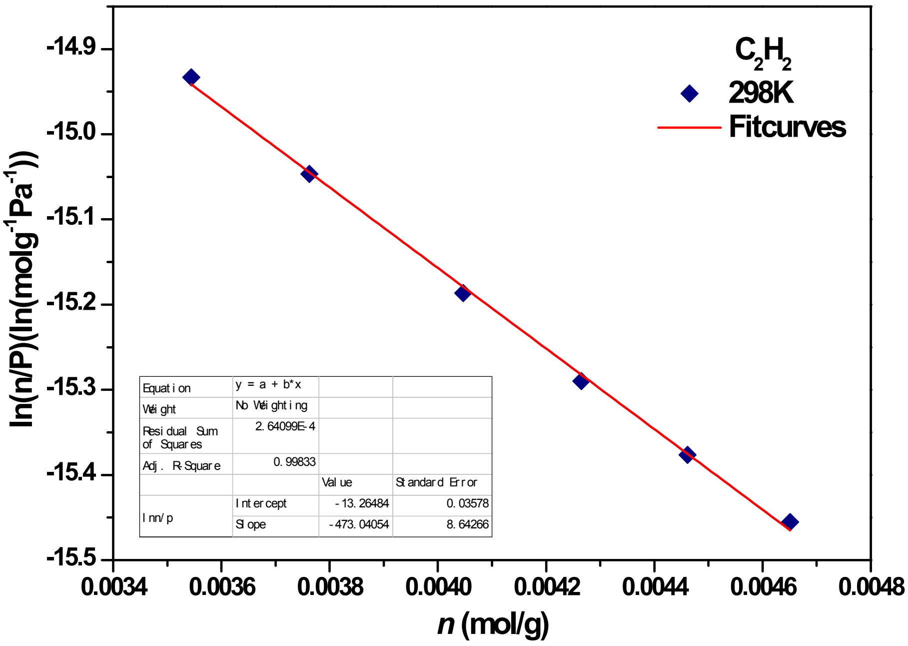

Figure S28. Virial analysis of the adsorption data for C_2H_2 on Cu-TDPAT at 298 K: Low pressure data.

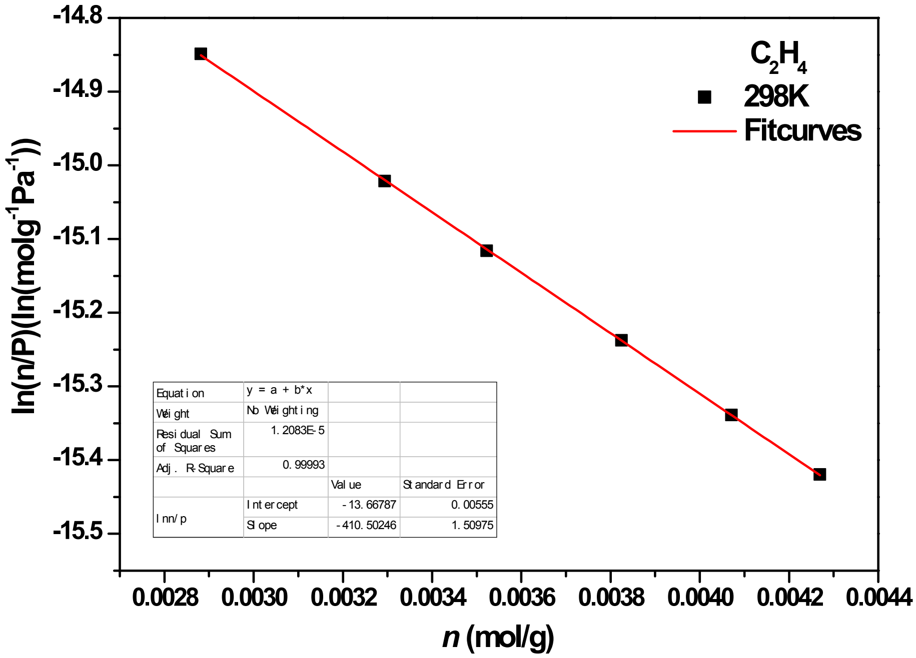

Figure S28. Virial analysis of the adsorption data for C_2H_4 on Cu-TDPAT at 298 K: Low pressure data.

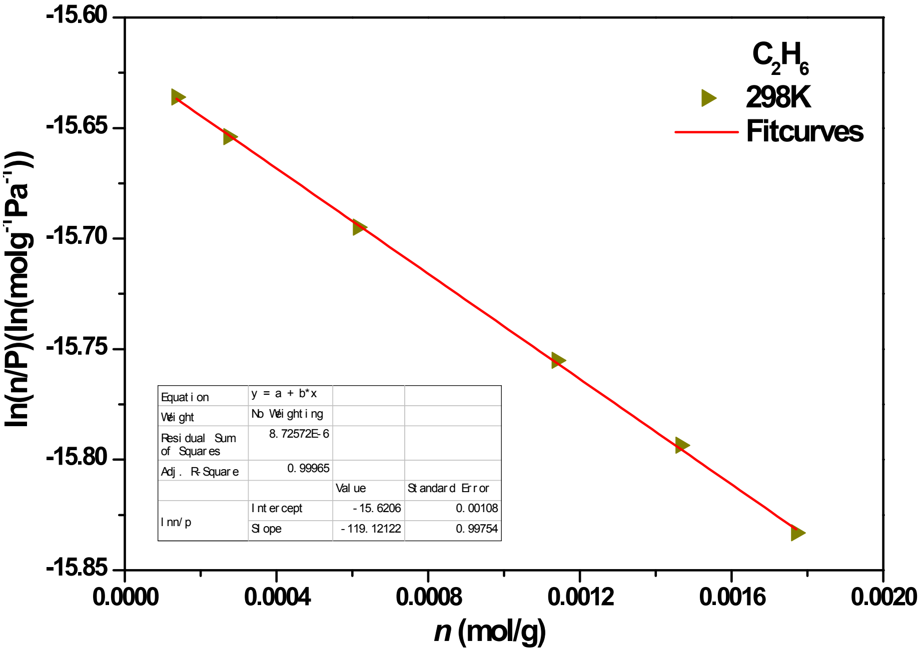

Figure S28. Virial analysis of the adsorption data for C_2H_6 on Cu-TDPAT at 298 K: Low pressure data.

Section VI. Breakthrough experiments

The breakthrough separation experiments were conducted at 298 K on a homemade apparatus. Detailed information of the setup can be found in our previous publication.[3] In a typical experiment, 500 mg of porous sorbent was thoroughly ground and packed into a quartz column (5.8 mm I.D. × 150 mm) with silica wool filling the void space. The sorbent was in situ activated in the column with a helium flow (10 cm^3 min^{-1}) at 393 K for 1 h before the temperature of the column was decreased to 298 K. The flow of He was then turned off while a dry gas mixture at 10.0 cm^3 min^{-1} was sent into the column. The effluent from the column was monitored using a GC with a flame ionization detector (GC-FID) or mass spectrometer (MS). The dead volume was determined using the same column after adsorption saturation.

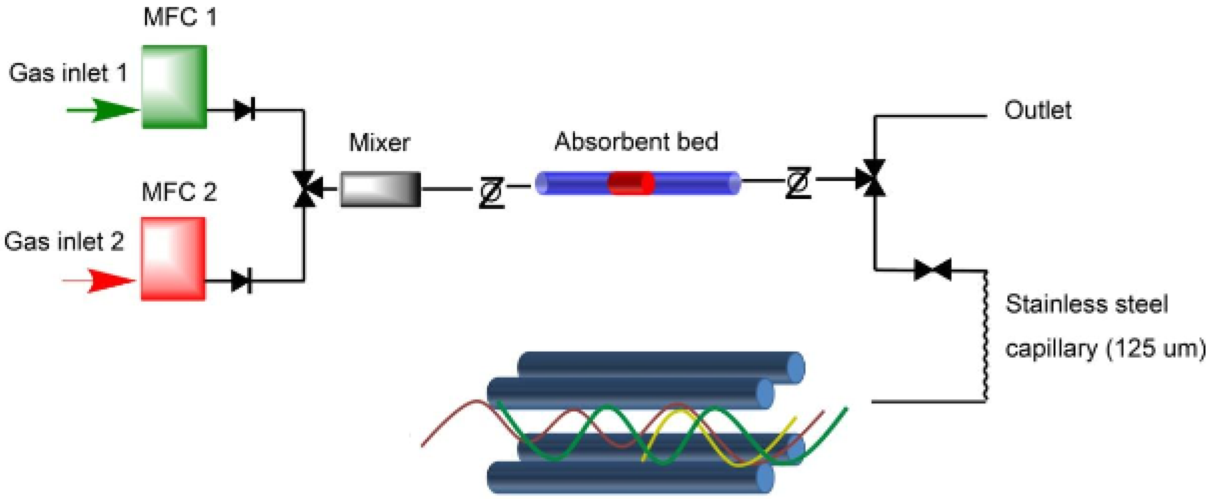

Figure S29. Schematic illustration of the apparatus used for the breakthrough experiments.

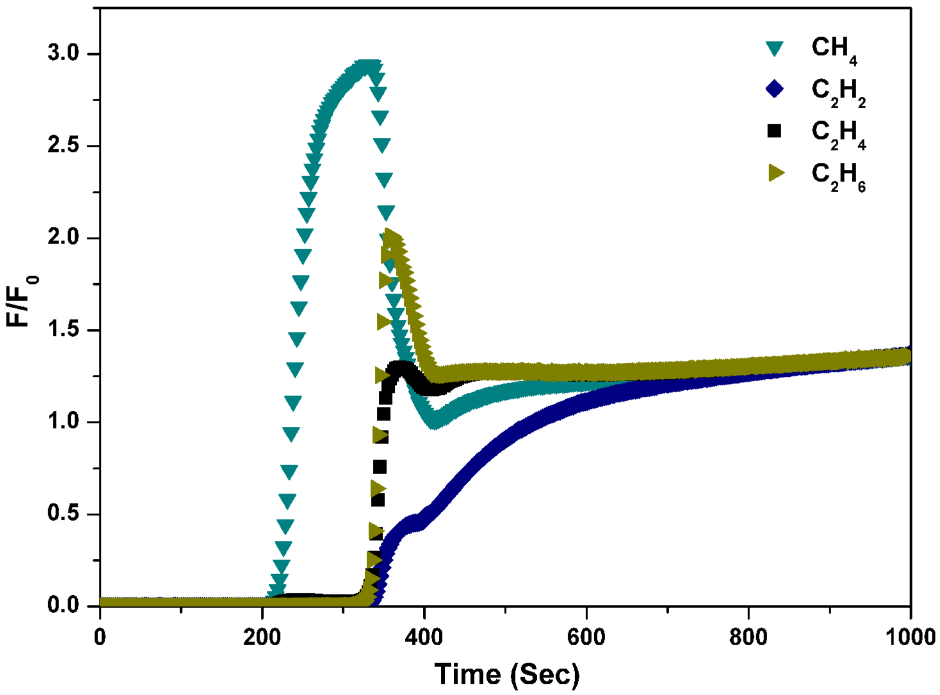

Figure S30. Column breakthrough experiment (Run 1) in Cu-TDPAT.

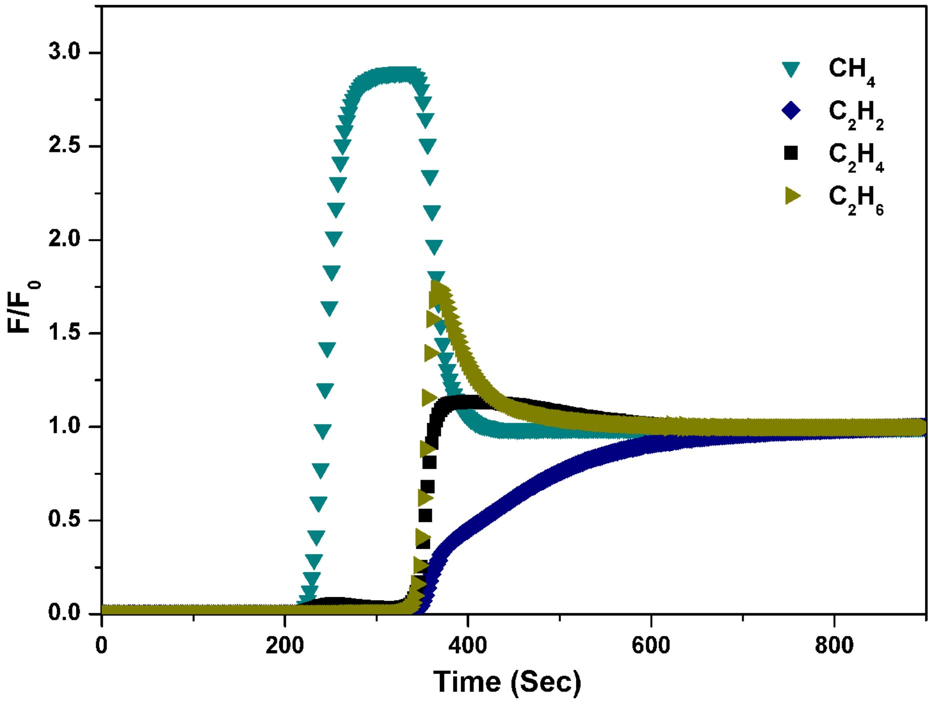

Figure S31. Column breakthrough experiment (Run 2) in Cu-TDPAT.

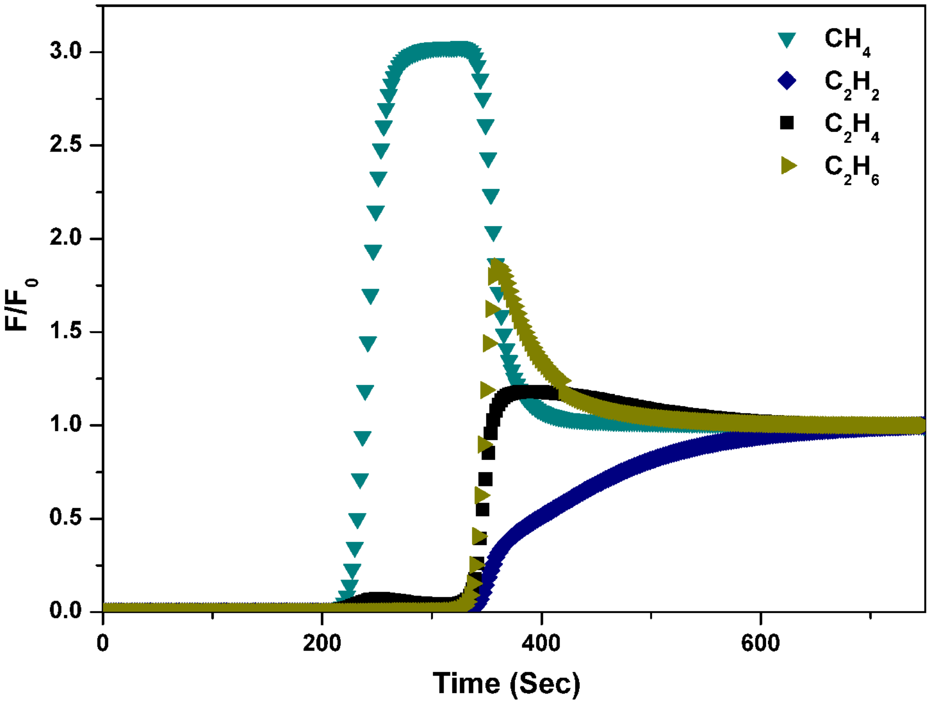

Figure S32. Column breakthrough experiment (Run 3) in Cu-TDPAT.

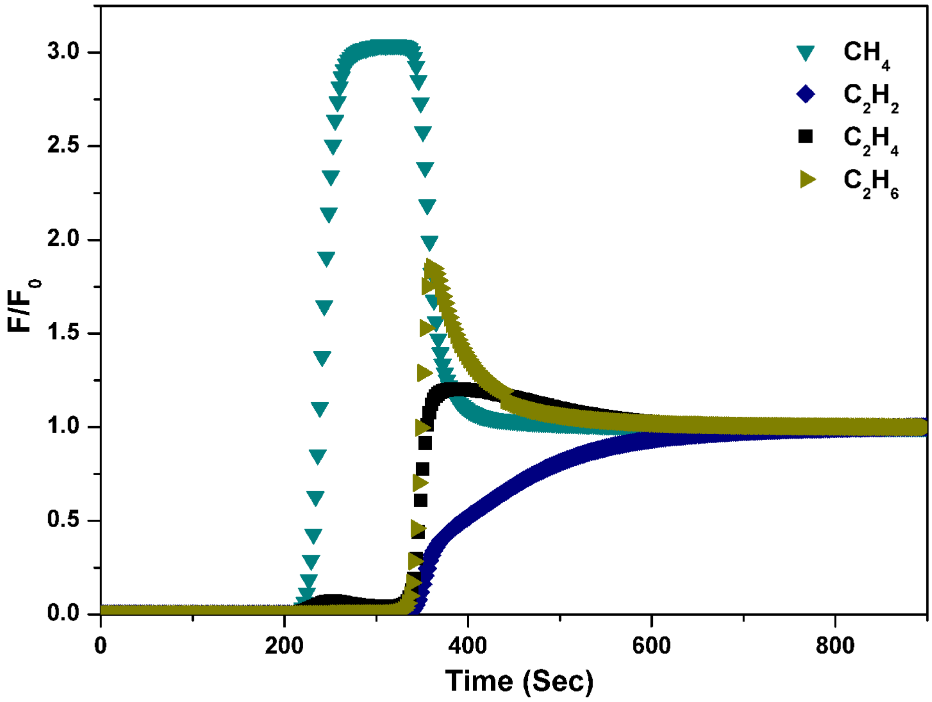

Figure S33. Column breakthrough experiment (Run 4) in Cu-TDPAT.

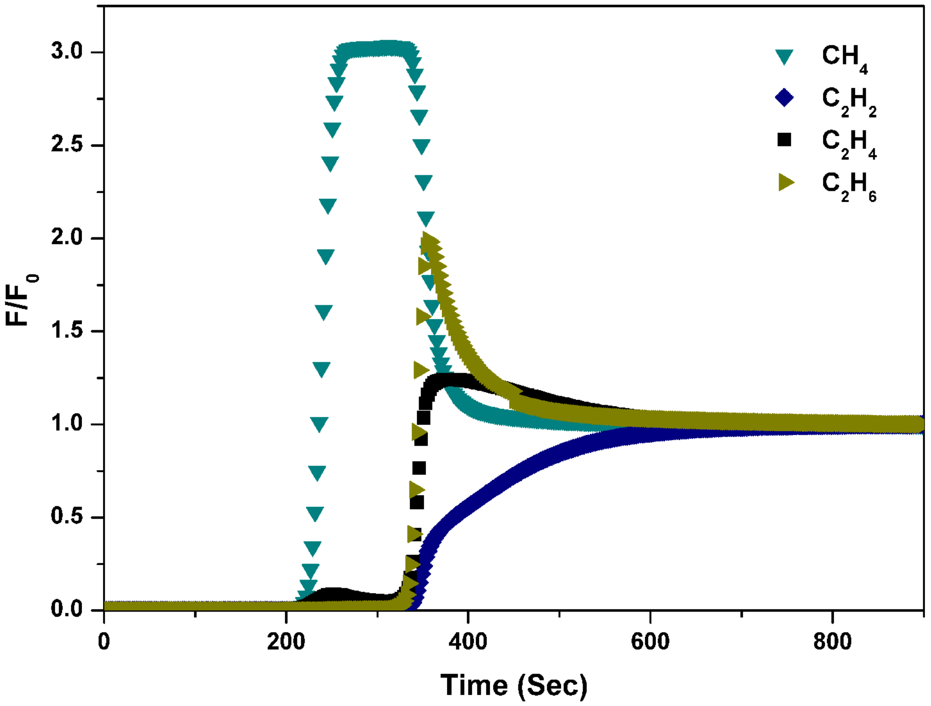

Figure S34. Column breakthrough experiment (Run 5) in Cu-TDPAT.

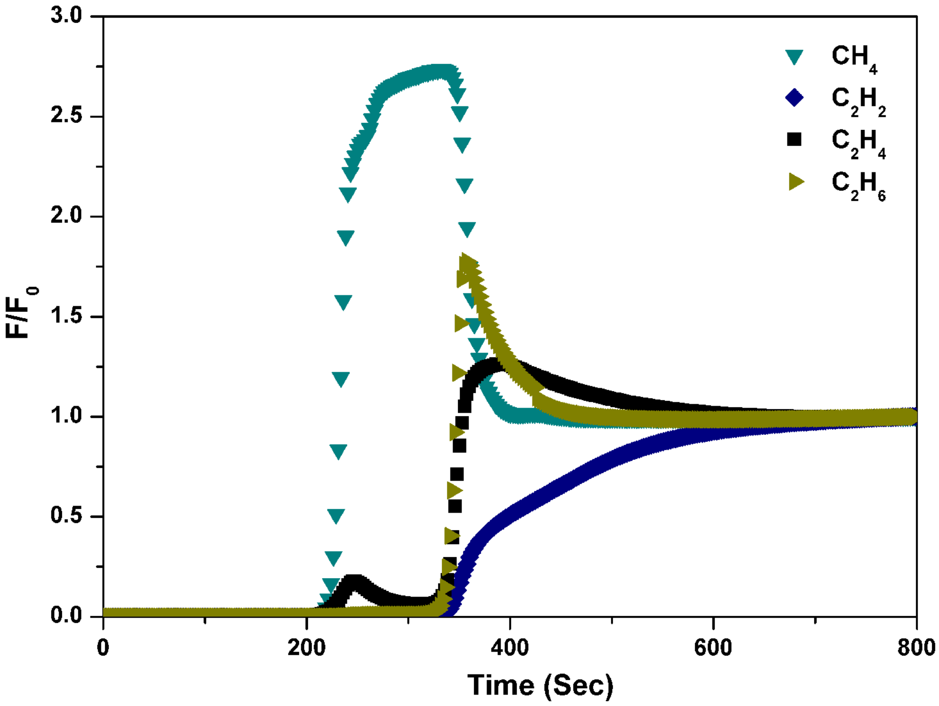

Figure S35. Column breakthrough experiment (Run 6) in Cu-TDPAT.

Section VII. Theoretical calculations

All calculations were performed with the Perdew−Burke−Ernzerhof (PBE) exchange-correlation functional and the double numerical plus polarization basis set using the program DMol3.[12] The cluster models representing the Cu cluster and the ligand were cut from the single-crystal structure and saturated by dangling H atoms. C2 molecules were manually put close to the Cu cluster and ligand, respectively. Geometry optimizations were performed with all non-H atoms in the cluster models fixed. Different C2 configurations were tested, and the ones with the strongest host-guest interactions were saved.

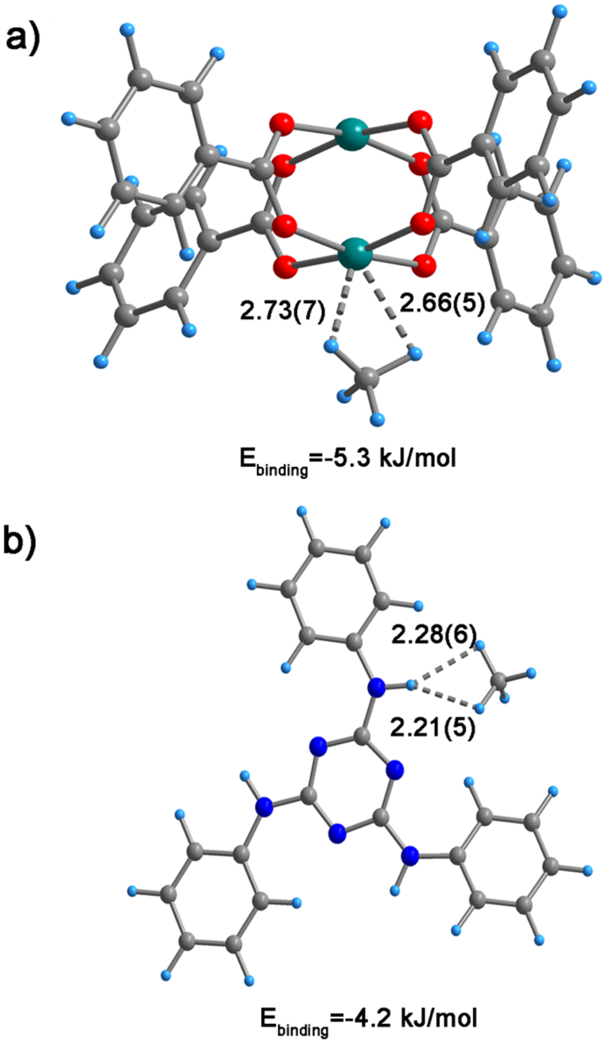

Figure S36. DFT optimized geometry for CH_4. Close contact distances, in Å, are marked. Green, red, gray, blue and light blue represent Cu, O, C, N and H atoms, respectively.

Table S1. Acetylene adsorption on some porous MOFs at room temperature and atmospheric pressure.

Material	BET (Langmuir) SA [$m^2\ g^{-1}$]	Pore volume [$cm^3\ g^{-1}$]	C_2H_2 uptake [$cm^3\ g^{-1}$]	Q_{st} [$kJ\ mol^{-1}$]	Ref.
HKUST-1	1401 (2095)	0.76	201	30.4	4
CoMOF-74	1018 (1504)	-	197	50.1	5
NOTT-101	(2930)	1.05	184	37.1	6
Cu-TDPAT	1938 (2608)	0.93	178	42.5	This work
PCN-16	(2810)	1.00	176	44.2	6
Cu_2(ebtc)	1852 (2844)	1.00	160	34.5	7
Cu-TDPAH	2171 (2540)	0.91	156	23.5	8
Cu_4L^a	1115 (1722)	0.61	154	-	9
ZJU-60a	1627 (2394)	0.87	151	17.6	10
UTSA-20	(1894)	0.67	150	30.8	6

[a] H_8L =tetrakis[(3,5-dicarboxyphenoxy)methyl]methane.

Table S2. Virial graph analysis data for **1** and separation selectivities of C_2 hydrocarbons and carbon dioxide over methane.

Adsorbate	T [K]	K_H [$mol\ g^{-1}Pa^{-1}$]	A_0 [$\ln(mol\ g^{-1}Pa^{-1})$]	A_1 [$gmol^{-1}$]	R^2	S_{ij} [a]	Q_{st} [$kJmol^{-1}$]
CH_4	273	2.935×10^{-8}	-17.344±0.000	-131.492±0.590	0.99990		20.7
	298	1.364×10^{-8}	-18.110±0.001	-126.910±2.158	0.99856		
C_2H_2	273	4.529×10^{-6}	-12.305±0.083	-432.204±17.631	0.99173	154.3	42.5
	298	1.734×10^{-6}	-13.265±0.036	-473.041±8.643	0.99833	127.1	
C_2H_4	273	3.660×10^{-6}	-12.518±0.040	-418.391±7.066	0.99858	124.7	49.5
	298	1.159×10^{-6}	-13.668±0.006	-410.502±1.510	0.99993	85.0	
C_2H_6	273	4.817×10^{-7}	-14.546±0.008	-141.468±1.710	0.99927	16.4	30.2
	298	1.644×10^{-7}	-15.621±0.001	-119.121±0.998	0.99965	12.1	

[a] The Henry's law selectivity for gas component i over CH_4 at the speculated temperature is calculated based on the equation: $S_{ij}=K_{H(i)}/K_{H(CH4)}$.

Table S3. The refined parameters for the Dual-site Langmuir-Freundlich equations fit for the pure isotherms of C_2H_2, C_2H_4, C_2H_6, CO_2 and CH_4 in **1** at 298 K.

	N_1^{max} [mmol/g]	b_1 [kPa^{-1}]	n_1	N_2^{max} [mmol/g]	b_2 [kPa^{-1}]	n_2	R^2
C_2H_2	1.619158	1.917854	0.675008	23.852281	0.023573	0.587391	0.999971
C_2H_4	4.202824	0.188869	0.763954	48.326749	0.005383	0.586646	0.999996
C_2H_6	2.788607	0.001236	1.677920	15.635443	0.021207	0.651757	0.999999
CH_4	1.711350	0.006581	0.847463	5.483669	0.000774	1.164892	0.999999

Table S4. Pore characteristics of Cu-TDPAT and Cu-TDPAH.

	Cu-TDPAT	Cu-TDPAH
L [Å] [a]	5.0	5.9
cub-Oh size [Å]	12	12
T-Td size [Å]	9.1	10.4
T-Oh size [Å]	17.2	17.2
BET SA [m^{2}g^{-1}]	1938	2171
Pore volume [cm^{3}g^{-1}] [b]	0.93	0.91
Total accessible volume [%] [c]	70.2	71.7
Density [g cm^{-3}]	0.782	0.775
OMS Density [per nm^3]	1.76	1.72
LBS Density [per nm^3]	3.5	5.4

[a] L is defined as the distance (Å) between the center of the ligand and the center of a terminal benzene ring. [b] Pore volumes were calculated from N_2 isotherms. [c] The total accessible volumes are calculated using the PLATON/VOID routine.[11]

References:

1. B. Li, Z. Zhang, Y. Li, K. Yao, Y. Zhu, Z. Deng, F. Yang, X. Zhou, G. Li, H. Wu, N. Nijem, Y. J. Chabal, Z. Lai, Y. Han, Z. Shi, S. Feng and J. Li, *Angew. Chem. Int. Ed.* 2012, **51**, 1412-1415.
2. J. L. C. Rowsell, O. M. Yaghi, *J. Am. Chem. Soc.*, 2006, **128**, 1304-1315.
3. (a) B. Li, Y. Zhang, R. Krishna, K. Yao, Y. Han, Z. Wu, D. Ma, Z. Shi, T. Pham, B. Space, J. Liu, P. K. Thallapally, J. Liu, M. Chrzanowski and S. Ma, *J. Am. Chem. Soc.*, 2014, DOI: 10.1021/ja502119z; (b) H. Wang, K. Yao, Z. Zhang, J. Jagiello, Q. Gong, Y. Han and J. Li, *Chem. Sci.*, 2014, **5**, 620-624; (c) Y. Zhao, K.Yao, B. Teng, T. Zhang and Y. Han, *Energy Environ. Sci.*, 2013, **6**, 3684-3692.
4. S. Xiang, W. Zhou, J. M. Gallegos, Y. Liu, B. Chen, *J. Am. Chem. Soc.*, 2009, **131**, 12415-12419.
5. S. Xiang, W. Zhou, Z. Zhang, M. A. Green, Y. Liu, B. Chen, *Angew. Chem., Int. Ed.*, 2010, **49**, 4615-4618.
6. Y. He, R. Krishna, B. Chen, *Energy Environ. Sci.*, 2012, **5**, 9107-9120.
7. Y. Hu, S. Xiang, W. Zhang, Z. Zhang, L. Wang, J. Bai, B. Chen, *Chem. Commun.*, 2009, 7551-7553.
8. K. Liu, B. Li, Y. Li, X. Li, F. Yang, G. Zeng, Y. Peng, Z. Zhang, G. Li, Z. Shi, S. Feng, D. Song, *Chem. Commun.*, 2014, **50**, 5031-5033.
9. Y. Xue, Y. He, S. Ren, Y. Yue, L. Zhou, Y. Li, H. Du, X. You, B. Chen, *J. Mater. Chem.*, 2012, **22**, 10195-10199.
10. X. Duan, Q. Zhang, J. Cai, Y. Yang, Y. Cui, Y. He, C. Wu, R. Krishna, B. Chen and G. Qian, *J. Mater. Chem. A*, 2014, **2**, 2628-2633.
11. A. L. Spek, PLATON: A Multipurpose Crystallographic Tool, Utrecht University, Utrecht, The Netherlands, 2001.
12. *Materials Studio*. San Diego, CA 92121, USA: Accelrys Software Inc., 2005.